ISSN 0023-1584, Kinetics and Catalysis, 2011, Vol. 52, No. 5, pp. 739–748. © Pleiades Publishing, Ltd., 2011.
Original Russian Text © N.A. Kurbatova, A.R. El'man, T.V. Bukharkina, 2011, published in Kinetika i Kataliz, 2011, Vol. 52, No. 5, pp. 753–763.

Application of Catalysts to Coal Gasification with Carbon Dioxide

N. A. Kurbatova[a], A. R. El'man[a], and T. V. Bukharkina[b]
[a] *OOO Rostkhim, Moscow, Russia*
[b] *Mendeleev University of Chemical Technology of Russia, Moscow, 125047 Russia*
e-mail: nkurbatova_laboratory@mail.ru

Received August 30, 2010

Abstract—The effects of the additives of iron, nickel, zinc, and their oxides on the process of coal gasification with carbon dioxide at temperatures of 550–800°C was studied. It was found that the additives used did not exhibit noticeable activity upon mixing with coal. Impregnation with nickel was found most efficient; it caused a notable increase in the rate of the process and a higher degree of CO_2 conversion, as compared with the thermodynamically equilibrium conversion for a given temperature. Thus, impregnation with 5% nickel made it possible to decrease the reaction temperature by 80°C with the retention of the yield of CO at about 100%. Kinetic models for describing noncatalytic and catalytic gasification reactions were considered and a mechanism of the process in the presence of nickel was proposed.

DOI: 10.1134/S0023158411050090

INTRODUCTION

Carbon monoxide is one of the most important raw materials for chemicals production: 75% acetic acid (world production of ~5 million tons per year) [1] is manufactured by the carbonylation of methanol. Recently, the role of CO as a chemical raw material, in particular, for the production of metal carbonyls, synthetic fatty acids, isocyanates, alcohols, and fine organic synthesis products, has been especially increased because of a considerable increase and the instability of oil prices. However, the absence of an adequate technology for the production of pure carbon monoxide prevents the wide acceptance of carbonylation processes.

Currently available processes for the production of carbon monoxide are based on coal gasification with air or an air–steam mixture, methane conversion, methyl formate or methanol decomposition [2], and the membrane separation of synthesis gas. However, none of the above processes makes it possible to obtain pure CO; additional stages should be introduced for the separation and utilization of by-products and impurities (hydrogen, oxygen, methane, nitrogen, moisture, and methanol), and membrane technologies for the separation of synthesis gas remain expensive.

In recent years, the development of a wasteless technology for the production of CO by coal gasification with carbon dioxide (reverse Boudouard reaction) has been intensively studied in a number of countries:

$$C + CO_2 \leftrightarrow 2CO, \quad \Delta H_{298} = 176\,\text{kJ/mol}. \qquad \text{(I)}$$

In this case, carbon materials with high carbon contents (for example, activated carbon, anthracite, and pitch coke) should be used for the manufacture of high-quality CO.

This method is free of all of the disadvantages of the current industrial processes. The results of kinetic studies have been published [3–8]; the constructions of industrial reactors have been developed [9, 10], and various processes have been examined. Because the production of CO from CO_2 is of considerable interest due to the need for solving a problem of carbon dioxide utilization, it is not surprising that even exotic versions such as the use of solar energy for this purpose have been considered [11–15].

Recently, we have developed an original pilot plant with an output of no less than 2000 m^3/h [9], which makes it possible to obtain CO of 99% purity by the gasification of carbon materials with carbon dioxide. The production cost of CO is lower than the market price by a factor of almost 10. However, the required degree of CO purity (low residual CO_2 content) is reached only at sufficiently high temperatures, which require relatively high power consumptions, because of the reversibility of reaction (I).

At the same time, it is well known that the addition of metals or metal compounds to coal increases the rate of the process and makes it possible to more rapidly reach the equilibrium of reaction. As a rule, alkali or alkaline earth metal carbonates and also transition metals or their oxides serve as additives [8, 11–13, 16–23]. Significant catalytic effects were obtained with the use of zinc oxide [12, 19], iron [18, 24], iron oxide [12, 13, 21], nickel oxide [13, 18, 20], and nickel [21]. Considerable catalytic activity of cobalt was found [21, 25].

In our opinion, the manufacture of CO in molten metals or metal salts (potassium [23], sodium [17], and lithium [11, 23]) is unpromising from a technological point of view because of the problem of unloading the spent melt and utilizing large amounts of metal compounds. The process occurring in the presence of the mixtures of metal compounds with coal was mainly studied at very low degrees of coal and CO_2 conversion [12, 13, 18, 20]; because of this, the efficiency of catalysts used in the production of CO cannot be judged. Reactors of various designs were used to perform this process: fixed-bed [13, 19–21] and fluidized-bed reactors [12, 24], and also a mixing reactor [18]. The reaction conditions were often not comparable; because of this, the found regularities cannot be generalized and the most effective conditions for the production of target CO cannot be chosen. In many studies [11, 13, 16–18], large (not catalytic) amounts of metal compound additives were used; this is also unpromising for the industrial production of CO.

A number of publications were dedicated to study the kinetics and mechanism of the process of coal gasification under the action of CO_2 in the absence and in the presence of catalysts. It was found that the surface structure and porosity [5, 6, 21] and also the concentrations of mineral impurities [4, 5, 8, 26] exert a significant effect on the activity of gasified coal in an noncatalytic process. Fu and Wang [3] found a mathematical relationship between the energy parameters and the type of coal, its ash content, moisture content, and the concentrations of carbon and volatile components. It is assumed that the interaction of carbon dioxide with coal occurs through the carbon dioxide adsorption stage; the rate equation of the forward reaction corresponds to the Langmuir kinetics [5, 27].

In a number of publications, the mechanism of the catalytic action of additives was explained by the occurrence of the reaction through metal oxidation–reduction [8, 12, 13], for example, according to the reaction scheme

$$\begin{aligned} ZnO + C &= Zn_{(gas)} + CO, \\ Zn_{(gas)} + CO_2 &= ZnO + CO. \end{aligned} \quad \text{(II)}$$

It is also assumed that the reaction rate increases as a result of oxygen transfer by transition metals (oxides) without their oxidation [12, 21, 22]:

$$\begin{aligned} Fe_xO_y + CO_2 &\rightarrow Fe_xO_y(O) + CO, \\ Fe_xO_y(O) + C &\rightarrow Fe_xO_y + CO. \end{aligned} \quad \text{(III)}$$

Moreover, the role of metal carbide formation in the increase in the rate of metal carbide gasification was noted [21].

The mechanism of the Boudouard reaction in the presence of sodium carbonate was studied with the use of reagents labeled with the ^{13}C isotope [16]. It was found that the catalytic action includes two stages: the reversible oxidation of a catalyst and its irreversible reduction. The resulting CO decreases the number of surface oxide centers and thus inhibits the process. However, the kinetics of the process was studied under nonisothermic conditions; therefore, the results obtained cannot be used, for example, for designing an industrial reactor.

Although a large body of experimental data on the catalytic gasification of coal with carbon dioxide has been accumulated, attempts at obtaining a reliable kinetic model of the process suitable for calculating an industrial reactor have almost not been made. Kodama et al. [12] derived a rate equation for the consumption of coal in its gasification when it is impregnated with In, Zn, and Fe oxides. However, the model proposed does not describe the processes of CO_2 consumption and CO formation and does not consider the role of a metallic catalyst.

In our opinion, use of porous carbon materials impregnated with metal compounds is of the greatest interest for the production of CO because impregnation provides the best contact and distribution of a catalyst in a carbon grain. The aim of this work was to study the kinetics of coal gasification with carbon dioxide in the absence and in the presence of metal (Ni, Fe, and Zn) compounds, to search for the most active catalysts, and to obtain a kinetic description of the process taking into account forward and reverse reactions up to the deep degrees of CO_2 conversion suitable for calculating a reactor.

EXPERIMENTAL

BAU-A activated carbon (GOST [State Standard] 6217-74), carbon dioxide (superior quality, GOST 8050-85), nickel(II) nitrate hexahydrate (reagent grade, GOST 4055-78), iron(III) nitrate nonahydrate (from Scharlau), zinc(II) nitrate hexahydrate, zinc oxide (reagent grade), PTsR-1 zinc powder (TU [Technical Specifications] 1721-015-12288779-2002), and carbonyl nickel (powder) were used in this study.

The reaction was performed in a vertical reactor with a fixed bed of carbon. Carbon dioxide was supplied from the top to exclude the separation of carbon and metal powder because of different densities of these materials. The residence time of a gas in the reactor was regulated by changing the input flow rate of CO_2. The gas from the reactor outlet was analyzed on a gas chromatograph with a thermal conductivity detector using a steel chromatographic column 3 m in length and 3 mm in diameter packed with activated carbon of 60–80 mesh. The conditions of chromatographing were as follows: detector current, 105 mA; detector temperature, 100°C; carrier-gas (helium) flow rate, 30 ml/min; and injected sample volume (sample loop), 0.866 ml. The column oven temperature was maintained at 50°C for 2 min and then increased to 200°C at a rate of 25 K/min.

The state of carbon impregnated with a metal was determined by X-ray diffraction (XRD) analysis on a DRON-3 automated X-ray diffractometer. The analysis was performed using monochromated CuK_α radia-

Table 1. Material balance for the process of noncatalytic coal gasification

Before the onset of reaction			After the completion of reaction		
component	weight, g	number of moles	component	weight, g	number of moles
Carbon dioxide	19.42	0.441	Carbon dioxide	16.74	0.381
Carbon	1.58	0.132	Carbon monoxide	3.33	0.119
			Carbon	0.90	0.075
Total	21.00	0.573	Total	20.97	0.575

Note: Process conditions: temperature, 800°C; CO_2 flow rate, 3 l/h; contact time, 8.5 s; experiment time, 162 min.

tion in the range of 2θ angles from 10° to 115° at a step of 0.1° and a 4-s exposure at a measurement point. The spectra were processed and interpreted with the use of a program package developed at the Department of Physical Materials Science of the Moscow Institute of Steel and Alloys [28]. In the study of the effect of additives on the gasification process, we either used a mixture of carbon with a metal or metal oxide powder or impregnated carbon with a metal or metal oxide. Before the experiments, carbon was dried in a drying oven for 3 h at a temperature of 250°C.

Metals and metal oxides were deposited onto carbon by impregnation with aqueous solutions of $Zn(NO_3)_2 \cdot 6H_2O$, $Ni(NO_3)_2 \cdot 6H_2O$, and $Fe(NO_3)_3 \cdot 9H_2O$. The predried carbon was added to a metal salt solution so that the carbon layer was completely coated with the solution. Then, the resulting mixture was kept in a drying oven for 3 h at 100°C to remove moisture. Thereafter, the nitrate–impregnated carbon was calcined at 350°C for 3 h in a flow of nitrogen. Under these conditions, according to XRD data, zinc nitrate decomposed to ZnO, and iron nitrate decomposed to an $Fe_3O_4 \cdot Fe_2O_3$ oxide mixture in a molar ratio of 3 : 2; nickel nitrate was converted into nickel metal. We determined the nature of the impregnating additive using XRD analysis and calculated its weight based on the weight of the starting salt.

Before the onset of kinetic experiments, we determined the limits of the occurrence of noncatalytic and catalytic coal gasification reactions in external and internal diffusion regions. For this purpose, we experimentally determined at which rate of CO_2 consumption the rate of reaction ceased to depend on it at a maximum temperature used. In this case, the residence time was retained constant by changing the height of a carbon bed. We also determined the carbon particle size at which the rate of the process did not depend on it. At the flow rates of CO_2 greater than 0.5 l/h and a carbon particle size smaller than 1.6 mm, both noncatalytic gasification processes and the gasification of carbon impregnated with 5% Ni occurred in the kinetic region and did not experience internal and external diffusion limitations. To perform kinetic experiments, we used a carbon fraction with a particle size of 0.315–0.700 mm, and the rate of CO_2 consumption varied from 0.5 to 12 l/h. The initial concentration of CO_2 was changed using the previously prepared mixtures of CO_2 with nitrogen. The experimental data were processed using numerical integration (MODELU) and optimization (OPTIMD) programs developed at the Mendeleev University of Chemical Technology of Russia.

RESULTS AND DISCUSSION

In the preliminary experiments, we found that CO is the only reaction product and determined the material balance of the process (Table 1) under the following standard conditions: temperature, 800°C; CO_2 supply flow rate, 3 l/h; contact time, 8.5 s; and experiment time, 162 min. Data in Table 1 suggest a good precision of the material balance; the imbalance was no higher than 0.4%. Thus, the reaction stoichiometry satisfies Eq. (I).

The kinetics of noncatalytic reaction was studied in a series of experiments by changing the residence time and concentration of CO_2 at the reactor inlet (Fig. 1a). In this case, the degree of carbon conversion was no higher than 10% (an excess method). At this low degree of conversion, the decrease in the carbon surface area can be ignored and the concentration of CO_2 remained almost constant at a constant flow rate.

Figure 1a indicates that an equilibrium state was not reached in the experiments, although the residence time varied over a wide range. For determining equilibrium concentrations in noncatalytic reaction, we used the mixtures of CO with CO_2 of different compositions and found the temperature at which reaction (I) changed from forward to reverse reaction for each particular mixture. However, the numerical values of equilibrium constants (I) were found much lower than the values calculated according published thermodynamic data [29] for graphite.

Based on the experimental results, we selected kinetic model (1) using a method of the discrimination of kinetic models constructed on the basis of different hypotheses on the mechanism of the process. This

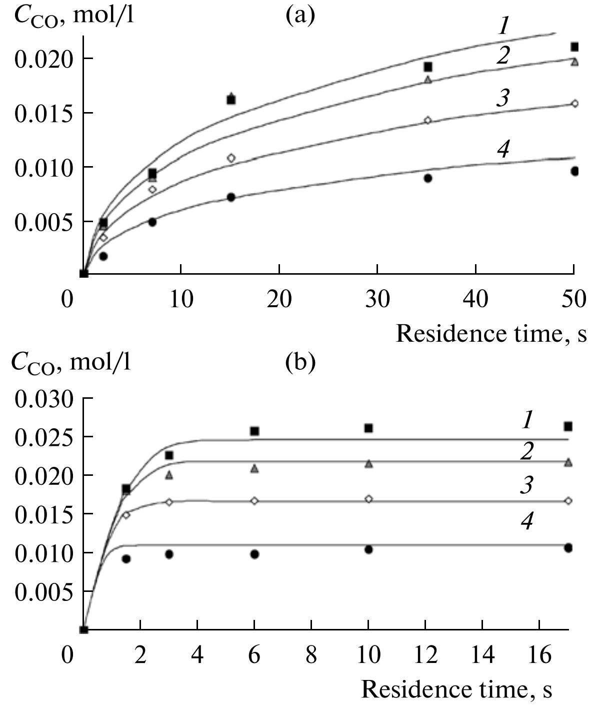

Fig. 1. Kinetics of CO formation at various initial concentrations of CO_2 (in mol/l). (a) Noncatalytic reaction (840°C): (*1*) 0.042, (*2*) 0.032, (*3*) 0.020, and (*4*) 0.010. (b) Catalytic reaction (700°C; 5% Ni/C): (*1*) 0.042, (*2*) 0.033, (*3*) 0.020, and (*4*) 0.010. Points and lines indicate experimental data and the results of calculations based on models (a) (*1*) and (b) (*2*), respectively.

model implies the physical adsorption of CO and CO_2 and the occurrence of the reverse reaction by the interaction of the adsorbed CO molecule with the CO molecule from the gas phase:

$$\frac{dC_{CO}}{d\tau} = k_1 \frac{C_{CO_2}}{1 + bC_{CO_2} + b'C_{CO}} - k_{-1} \frac{C_{CO}^2}{1 + bC_{CO_2} + b'C_{CO}}, \quad (1)$$

where k_1 is the rate constant of the forward reaction (s^{-1}); k_{-1} is the rate constant of the reverse reaction ($l\ s^{-1}\ mol^{-1}$); C_{CO_2} and C_{CO} are the concentrations of CO_2 and CO (mol/l), respectively. Taking into account the coefficient of an increase in the volume in accordance with the stoichiometry of reaction (I), we obtained a good agreement of the results of calculations according to this model with the experimental data (Fig. 1a).

Table 2. Kinetic parameters of noncatalytic reaction

Constant	E_{act}, kJ/mol	$\ln k_0$
k_1	337	35.58
b	30	6.77
k_{-1}	43	5.65
b'	82	16.40

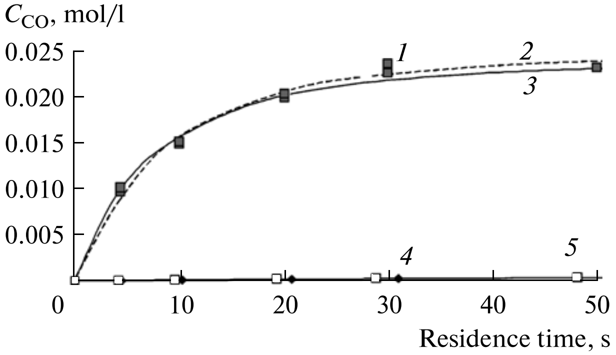

Fig. 2. Effects of the addition (by mixing) of zinc, zinc oxide, and nickel to carbon on the process of carbon dioxide gasification: (*1*) with no additives, 800°C; (*2*) 10% Zn, 800°C; (*3*) 10% ZnO, 800°C; (*4*) no additives, 600°C; and (*5*) 10% Ni, 600°C.

For determining the kinetic parameters of the process examined, we obtained the experimental dependence of C_{CO} on the residence time τ at $C_{CO_2,0} = 0.042$ mol/l (100%) in the temperature range of 800–1000°C (Table 2). By the mathematical treatment of this dependence according to model (1), we calculated the activation energy (E_{act}) and frequency factor (k_0). The found activation energy (Table 2) is consistent with published data [3–5, 8, 16, 21, 27].

The effect of metal or metal oxide powder additives to carbon on the process of the production of CO was studied at temperatures of 600 and 800°C. Figure 2 shows that the catalytic effect was almost absent upon mixing nickel, zinc, and zinc oxide powders with carbon. This is likely due to the fact that, under the selected conditions, mixing did not provide necessary contact between carbon and catalyst particles. Better contact was, apparently, achieved in studies [12, 18], where reactors of other types were used (a ball mill and a fluidized-bed reactor). Yamada et al. [20] noted a catalytic effect upon mixing nickel metal with carbon; however, this occurred only at higher temperatures than those used in this work (Fig. 2).

Carbon impregnated with iron oxides exhibited an insignificant activity, whereas ZnO was found inactive at all (Fig. 3a).

Figure 3b is indicative of a rapid loss of activity in iron oxides in the course of the process: the formation of CO ceased at the carbon conversion $x_a = 1\%$; in this case, the catalyst turnover number was only 1–2. The carbon conversion was calculated from the equation

$$x_a = \frac{m_{C,0} - m_C}{m_{C,0}} \times 100,$$

where $m_{C,0}$ is the initial weight of coal, and m_C is the current weight of coal calculated in accordance with the amount of formed CO.

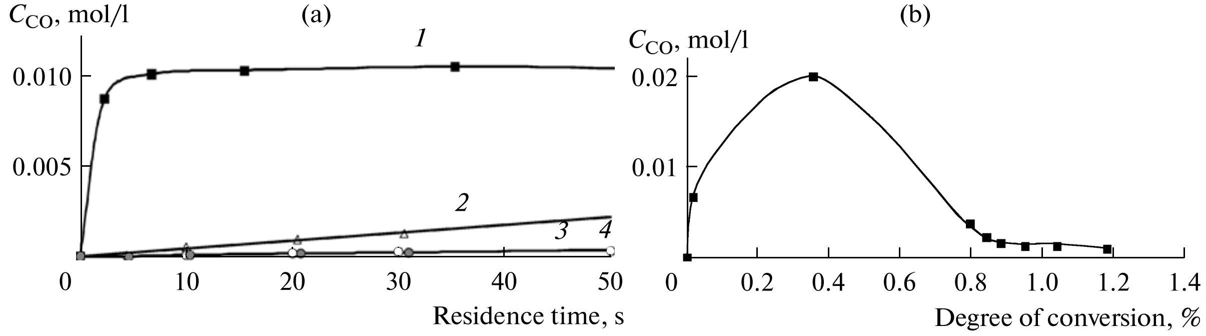

Fig. 3. Effects of impregnation with catalysts on the coal gasification process at 600°C: (a) (*1*) 5% Ni, (*2*) 10% (Fe_2O_3 + Fe_3O_4), (*3*) 10% ZnO, and (*4*) no additives; (b) 10% (Fe_2O_3 + Fe_3O_4); CO_2 flow rate, 10 l/h (non-steady-state conditions).

The experimental results suggest that, in the initial period of reaction, a relatively large amount of CO was released in the course of a rapid process, which soon terminated; it is likely that a small catalytic effect was observed in the subsequent gasification. DeGroot and Shafizadeh [8] found that the catalyst impregnated with iron oxides exhibited a significant activity, which decreased very rapidly; however, it can be restored by heating in a flow of nitrogen. According to current concepts, the catalytic process can occur in accordance with reaction schemes (III) [12] or (IV) [13]:

$$\begin{gathered} Fe_3O_4 + C \rightarrow 3FeO + CO, \\ 3FeO + CO_2 \rightarrow Fe_3O_4 + CO. \end{gathered} \tag{IV}$$

In our experiments, the initial impregnated sample contained iron in the forms of both Fe(III) (Fe_2O_3) and the mixed oxide of Fe(II) and Fe(III) (Fe_3O_4) (see Experimental), and only Fe_3O_4 was detected in it after the completion of the process. Therefore, it is believed that Fe(III) is much more active than Fe(II), but it is converted into Fe_3O_4 in the course of gasification and the catalyst activity sharply decreases:

$$\begin{gathered} Fe_2O_3 + C \rightarrow 2FeO + CO, \\ 2FeO + CO_2 \rightarrow Fe_2O_3 + CO, \\ Fe_2O_3 + FeO \rightarrow Fe_3O_4. \end{gathered} \tag{V}$$

After this, the catalytic system operates under steady-state conditions to exhibit a comparatively low activity (Fig. 3a).

Gokon et al. [19] noted a noticeable activity of samples impregnated with zinc oxide (to 7 l h^{-1} g_C^{-1} at 800°C); however, this activity almost completely disappeared after 60% carbon conversion (30 min after the beginning of the experiment). This activity can be caused by the higher temperature of the calcination of deposited zinc nitrate and by the additional crushing of carbon after impregnation with ZnO. In our experiments, deposited zinc oxide not only did not accelerate the process of coal gasification (Fig. 3a) but also inhibited the formation of CO at high concentrations (above 10%) and elevated temperatures (800°C). The decrease in the yield of CO can be explained by either the possible blocking of active centers on the carbon surface of coal by ZnO molecules or an increase in the rate of the well-known [14, 30, 31] reversible reaction

$$ZnO + CO \leftrightarrow CO_2 + Zn. \tag{VI}$$

It is likely that catalysts based on iron and zinc will exhibit higher activity at higher temperatures and also with the use of other methods of impregnating or activating these metals.

However, samples impregnated with nickel are of greatest interest. The introduction of 1 wt % nickel allows one to increase the initial rate of reaction at 600°C by a factor of almost 12000 (as compared using models (1) and (2)) and to afford a much higher concentration of CO than that in the absence of nickel at the same residence times (Fig. 4). As the residence time was increased, the concentration of CO at the reactor outlet reached a steady-state value, which did not depend on the concentration of nickel (Fig. 4). It is likely that this steady-state concentration is an equi-

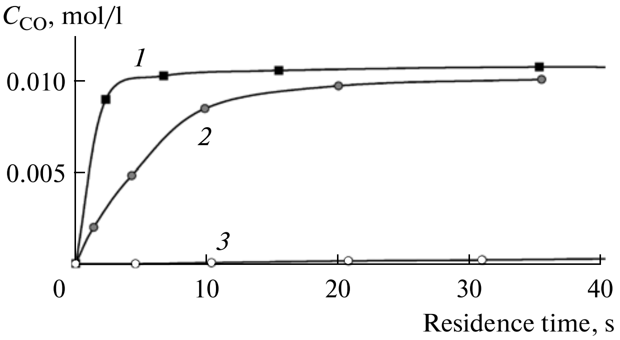

Fig. 4. Effect of impregnation with nickel on the coal gasification process at 600°C: (*1*) 5% Ni, (*2*) 1% Ni, and (*3*) no additives.

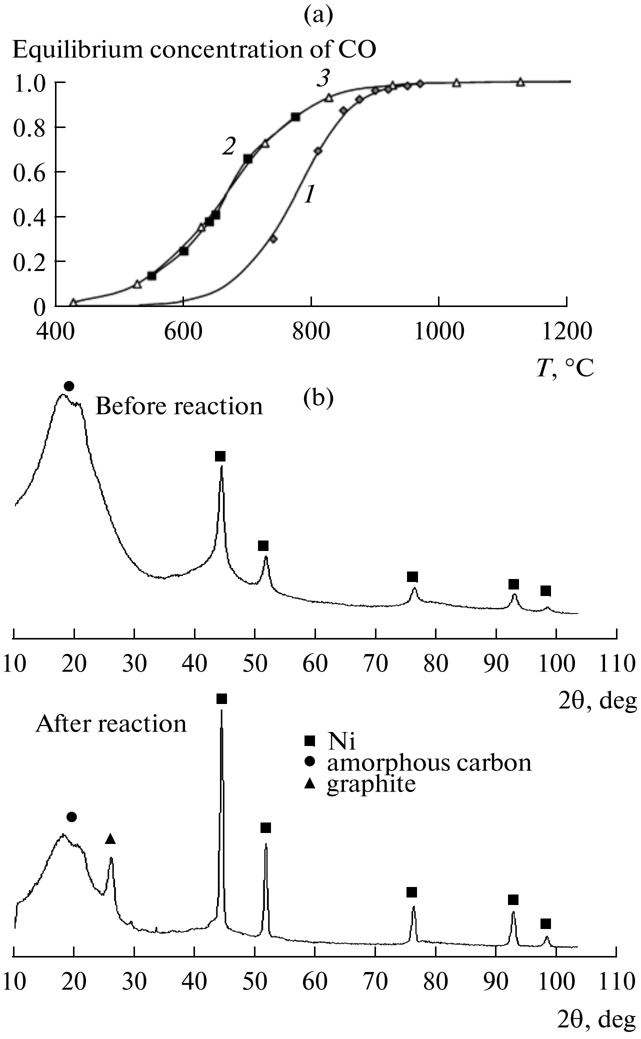

Fig. 5. (a) The temperature dependence of the concentration of CO in the gasification of carbon materials with carbon dioxide: (*1*) BAU-A carbon with no catalyst (experimental data), (*2*) BAU-A carbon impregnated with nickel (5% Ni/C; experimental data), and (*3*) thermodynamic calculation for graphite. (b) Detection of a graphite phase by XRD analysis after impregnation with nickel and upon performing the gasification of BAU-A carbon (800°C; 9.7% Ni/C).

librium concentration because the concentration of CO reached the same value upon performing reverse reaction (I) in the presence of nickel. However, the rate of reverse reaction (I) then rapidly decreased, probably, as a result of the carbonization of catalyst particles.

To test the thermodynamic state of the reaction system, we compared the experimentally found equilibrium concentrations of CO at different temperatures in the absence and in the presence of nickel with the results of thermodynamic calculations (Fig. 5a). The equilibrium concentrations of CO under conditions of coal gasification were determined based on the numerical values of the equilibrium constants K_p of reaction (I) at different temperatures: $K_p = \frac{P^2_{CO,eq}}{P_{CO_2,eq}}$, where $P_{CO,eq}$ and $P_{CO_2,eq}$ are the equilibrium pressures of CO and CO_2, respectively. K_p values at different temperatures were found from the equation $RT \ln K_p = -\Delta_r G^0_T$, where $\Delta_r G^0_T$ is the free enthalpy of reaction and R is the gas constant (8.314 J mol^{-1} K^{-1}). $\Delta_r G^0_T$ was calculated using the Temkin–Shvartsman method [29]. Note that the published values of $\Delta_f H^0_{298}$ and S^0_{298} (a change in the enthalpy upon formation from the elements under standard conditions and a standard change in the entropy, respectively) refer to graphite, whereas we used BAU-A carbon in our experiments.

Figure 5a shows that the experimentally measured equilibrium fractions of CO in an noncatalytic process of the gasification of BAU-A carbon (curve *1*) were lower than the values calculated for graphite on the basis of thermodynamic data (curve *2*). This can be explained by the nonzero value of the heat of formation of amorphous BAU-A carbon. At the same time, when BAU-A is impregnated with nickel, the equilibrium concentrations of CO reached upon gasification were higher than those in the noncatalytic reaction. In this case, the experimentally found equilibrium concentration of CO in the catalytic reaction coincided with the equilibrium concentration of CO calculated on the basis of thermodynamic data for graphite (curves *2* and *3* coincided). Because the catalyst cannot shift an equilibrium, in our case, a change in the equilibrium concentrations of CO and CO_2 can be caused by the formation of new phases in the system, including regular carbon structures. Thus, nickel immobilized on porous carbon considerably decreased the temperature at which an equilibrium concentration of CO comparable with that observed in the noncatalytic gasification of BAU-A. Obviously, another much more effective process of carbon dioxide coal gasification occurred in the presence of the catalyst, and the nature of this process should be specially studied.

We calculated the material balance for the catalytic reaction. As in the noncatalytic process, CO was the only gaseous reaction product. The weight of deposited nickel was calculated based on the weight of nitrate in the impregnating solution. The reaction was performed under the following conditions: temperature, 800°C; CO_2 flow rate, 12 l/h; contact time, 2 s; and experiment time, 66 min. After performing the reaction, carbon was combusted in an atmosphere of CO_2, and the weight of nickel after the reaction was calculated from the weight of the residue with a correction for the ash content of carbon. The ash content of the initial carbon was also determined by the combustion of a weighed portion of BAU-A in a flow of CO_2.

Data in Table 3 suggest a good precision of the material balance; the imbalance did not exceed 0.5%.

Table 3. Material balance for the process of catalytic coal gasification

Before the onset of reaction			After the completion of reaction		
component	weight, g	number of moles	component	weight, g	number of moles
Carbon dioxide	23.94	0.544	Carbon dioxide	22.99	0.522
Carbon	1.01	0.084	Carbon monoxide	1.22	0.044
			Carbon	0.71	0.059
Nickel	0.11	0.002	Nickel	0.10	0.002
Total:	25.06	0.630	Total:	25.02	0.627

Note: Process conditions: temperature, 800°C; CO_2 flow rate, 12 l/h; contact time, 2 s; and experiment time, 66 min.

Thus, the stoichiometry of the catalytic reaction is also consistent with Eq. (I).

We also derived an adequate rate equation for the catalytic reaction. Figure 1b shows the kinetic curves for the formation of CO at a temperature of 700°C and different initial concentrations of CO_2.

Based on the experimental data, we selected kinetic model (2) using a method of the discrimination of hypotheses concerning the mechanism of the process. This model assumed the physical adsorption of CO_2 and a second-order reverse reaction with respect to CO, when the molecule of adsorbed CO interacts with the molecule of CO from the gas phase:

$$\frac{dC_{CO}}{d\tau} = k_1 \frac{C_{CO_2}}{1 + bC_{CO_2}} - k_{-1} \frac{C_{CO}^2}{1 + bC_{CO_2}}. \qquad (2)$$

Gas concentrations calculated based on model (2) with consideration for the coefficient of volume change were consistent with the experimental data (Fig. 1b).

With the use of model (2), we calculated the kinetic parameters E_{act} and k_0 over the temperature range of 550–775°C (Table 4). For the samples impregnated with nickel, the activation energy of the forward reaction was lower than the E_{act} of the noncatalytic process by a factor of >1.5 (Table 2).

The results obtained suggest that, the samples impregnated with nickel metal, other processes occurred under the action of CO_2 than those in the absence of the metal, probably, with the participation of new phases. In this case, nickel, which was used in catalytic amounts, caused a noticeable rate of CO formation even at 0.05 at % (0.25% Ni/C). However, upon impregnation with 0.1 at % Ni (0.5% Ni/C), the catalyst turnover number was as high as 250 even at a 15% degree of carbon conversion, and the process occurred without inhibition. In special experiments, we found that the nickel catalyst stably operated up to high degrees of carbon conversion (to 40%). However, in the subsequent course of the process, the catalytic activity of nickel gradually decreased and the rate of gasification decreased to a level characteristic of noncatalytic reaction.

Because CO was the only gaseous reaction product and a material balance of the reaction was observed (Table 3), the change in the thermodynamics of the process can be caused by the appearance of new carbon phases, which were formed in the presence of a nickel catalyst and exhibited other thermodynamic characteristics than those of the initial amorphous BAU-A carbon. These phases can be formed both at the stage of carbon preparation and in the course of gasification; however, in any event, this caused a shift in the process equilibrium.

We did not detect the appearance of new crystalline phases up to the initial temperature of gasification upon heating the initial carbon sample impregnated with nickel in an atmosphere of nitrogen using XRD analysis, although it is well known [32] that fine-crystalline substances cannot be determined by this technique. However, a new phase with the reflection angle $2\theta = 26.1°$ (Fig. 5b) was found, which can correspond

Table 4. Kinetic parameters of catalytic reaction

Constant	E_{act}, kJ/mol	$\ln k_0$
k_1	196	29.32
b	148	27.83
k_{-1}	24	11.38

to graphite or carbon nanotubes [33]. The phase of graphite (or nanotubes) was also detected upon conducting the reverse reaction of CO disproportionation in the presence of the Ni/C impregnated catalyst. Therefore, it is possible to assume that graphite or nanotubes is a new carbon species that causes a shift of the equilibrium.

It is well known that carbon contacting with nickel is dissolved in it [32, 34, 35]. This makes possible the formation of carbon fibers and nanotubes [36–38], which can differ in diameter (from 10 to 10000 nm), morphology (straight or twisted), and the degree of graphitization. In this case, nickel serves as a catalyst. Tavares et al. [39] found that the value of $\Delta_r G_T^0$ in the gasification reaction of carbon fibers, which are formed upon the decomposition of CO on Ni, is 10–20 kJ/mol lower than that upon the gasification of graphite; this indicates a shift of the reaction equilibrium. Therefore, the role of nickel in the carbon dioxide gasification of BAU-A carbon can consist in the catalytic formation of new structures, for example, fibrous carbon structures [40] or nanotubes. It is well known that such processes proceed through the intermediate formation of nickel carbides [41]. Carbon fibers and nanotubes can undergo noncatalytic or catalytic (Ni) carbon dioxide gasification [12, 13, 21] with the formation of NiO_x oxides, whose interaction with carbon of nanotubes or fibers leads to the formation of CO.

Taking into account the above facts, we can propose the following version of the reaction scheme of the process:

(1) the formation of nanotubes and carbon fibers C_n at the stage of carbon preparation (the mechanism of this reaction was described in detail elsewhere [36, 41])

$$nC \xrightarrow{Ni} C_n; \qquad \text{(VII)}$$

(2) the noncatalytic gasification of the resulting carbon structure C_n

$$\begin{aligned} &C_n + CO_2 \leftrightarrow 2CO + C_{n-1},\\ &C_{n-1} + CO_2 \leftrightarrow 2CO + C_{n-2}; \end{aligned} \qquad \text{(VIII)}$$

(3) the catalytic gasification of C_n

$$\begin{aligned} &CO_2 + Ni \leftrightarrow NiO + CO\\ &NiO + C_n \rightarrow Ni + CO + C_{n-1}. \end{aligned} \qquad \text{(IX)}$$

Processes (VIII) and (IX) of noncatalytic and catalytic gasification, respectively, can occur until the quantitative conversion of the active form of carbon; thereafter, only low-activity amorphous carbon remains, and the rate of the process decreases to a level characteristic of the noncatalytic reaction.

Another possible explanation of the observed kinetics of the carbon dioxide gasification of carbon samples impregnated with nickel is the occurrence of coupled reactions. It is well known that the formation of regular carbon structures (graphite, carbon nanotubes, fibers, or filaments) on carbon contact with nickel results from the diffusion of dissolved carbon through the particles of nickel. This phenomenon was observed upon the interaction of various forms of carbon (nanotubes, carbon fibers, amorphous carbon, and carbon formed by the decomposition of CO and hydrocarbons) with Ni in a wide range of temperatures (600–1000°C), and quantitative characteristics (diffusion coefficients and activation energies [21, 35, 38, 41, 42]) were determined for a number of processes of this kind. Dissolved carbon after passing through the particles of nickel deposits on the surface of the solid carrier in the form of graphite [35] or another regular carbon structure [36, 41, 43], and it can undergo gasification at an interface between nickel and a gas phase in the presence of a gasifying agent [38, 42, 44]. In this case, it is likely that carbon released on the surface of nickel as a result of diffusion is in an atomic state and possesses a considerably higher activity in the gasification reaction. Therefore, the following coupled reactions can occur in the process: the formation of graphite (or another graphite-like material, for example, fibers and filaments) from amorphous carbon and the gasification of this carbon under the action of CO_2 through the intermediate active carbon particles C_{act}, which form on the metal surface as a result of the diffusion of dissolved carbon through nickel

$$\begin{aligned} &C \xrightarrow{Ni} C_{act},\\ &C_{act} \rightarrow C_{graphite},\\ &CO_2 + C_{act} \leftrightarrow 2CO. \end{aligned} \qquad \text{(X)}$$

Under the chosen conditions (at low temperatures), amorphous carbon does not react with CO_2; however, the occurrence of a coupled reaction of graphite formation with the participation of active carbon particles makes the gasification of coal possible. As is known [45], this coupling can shift the equilibrium of the main reaction, in this case, the carbon dioxide gasification of carbon.

The formation of graphite (reaction scheme (X)) can occur through intermediate nickel carbides Ni_xC_y [46]. In this case, in a number of publications [21, 38, 43, 47], carbide carbon was considered as the basic form of active carbon in reaction (I) catalyzed by impregnation with metal compounds. In our case, nickel carbide was not detected by XRD analysis; however, published data [46] suggest that it is in a metastable state over a wide range of temperatures and decomposes with the formation of graphite upon cooling. On the other hand, the absence of the NiO phase from carbon after the process can be explained by its rapid conversion (low surface concentration) in reduction with carbon (reaction scheme (IX)) or by high dispersity on the surface of carbon (analogously to published data [32]). At the same time, data obtained with the use of labeled $^{13}CO_2$ suggest the formation of NiO in the course of the carbon dioxide gasification of carbon [48].

The decrease in the rate of the process to a level characteristic of an noncatalytic reaction observed in our experiments can be not only a result of the complete conversion of active carbon species C_n at steps (VIII) and (IX) but also a consequence of the loss of contact between nickel and carbon and the termination of the formation of intermediate C_{act} compounds (reaction scheme (X)) or catalyst deactivation because of carbonization [21, 25, 49], oxidation, or growth of the metal particles. In addition, note that reaction mechanism (X) does not provide for the participation of NiO (which was not detected) and regular active carbon structures (nanotubes etc.), which can change the thermodynamics, in the gasification process. The thermodynamics can be changed by the coupled reactions of the formation of graphite from amorphous carbon and its gasification by carbon dioxide. The establishment of the nature of the active particles of carbon impregnated with nickel and also methods for carbon activation in the process of its carbon dioxide gasification will be the subject matter of our further studies.

The above results were obtained under quasi-steady-state conditions, when the degree of carbon conversion was no higher than 10%. However, unlike iron oxides (Fig. 3b), the nickel catalyst afforded a considerably higher degree of carbon conversion (to 40%); thereafter, the rate of gasification decreased to a level observed in the noncatalytic reaction. To regenerate the catalyst, spent carbon (1% NiC, 13.3 g) was treated with dilute nitric acid (80 ml, 35.7 g/l); in this case, nickel was converted into nitrate, which was then repeatedly precipitated from the resulting solution onto carbon (see Experimental). Thus, it was possible to partially restore the catalyst activity.

Based on the proposed kinetic models and the found numerical values of kinetic parameters, we can compare the efficiencies of the catalytic and noncatalytic processes of coal gasification under the action of CO_2. The calculations demonstrated that the impregnation of carbon with 5% nickel makes it possible to decrease the process temperature by 80°C with the retention of the same equilibrium concentration of CO and hence the same productivity of the process (Fig. 6). In this case, the prime cost of the product decreases because of decreasing reactor heating expenditures and also capital expenditures for the organization of the process.

Thus, use of the impregnation of carbon with the nickel catalyst makes it possible to considerably increase the reaction rate and process productivity. The catalytic effect was most pronounced at low temperatures, and this can be of considerable importance for conducting the low-temperature gasification of coal. At the same time, the found higher equilibrium concentrations of CO in the catalytic reaction, as compared with those in the noncatalytic reaction, together with the agreement of the temperature dependences of the equilibrium concentrations of CO in the catalytic reaction, on the one hand, and in the process of graphite gasification, on the other hand, require a further study of the mechanism of the process.

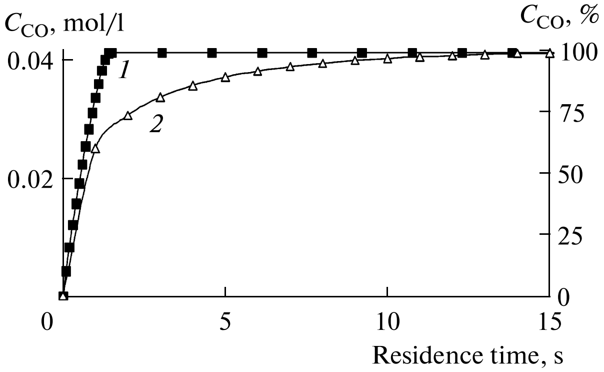

Fig. 6. Comparison between the efficiencies of catalytic (5% Ni/C; 970°C) and noncatalytic (1050°C) processes of carbon dioxide coal gasification (as calculated using models (*1*) and (*2*), respectively).

ACKNOWLEDGMENTS

We are grateful to Prof. O.N. Temkin and Cand. Sci. (Chem.) M.Yu. Sinev for helpful discussions of this work.

REFERENCES

1. Yoneda, N., Kusano, S., Yasui, M., Pujado, P., and Wilcher, S., *Appl. Catal., A*, 2001, vol. 221, p. 253.
2. *Khimicheskaya entsiklopediya* (Encyclopedia of Chemistry), Zefirov, N.S., et al., Eds., Moscow: Bol'shaya Rossiiskaya Entsiklopediya, 1999, vol. 5, p. 27.
3. Fu, W.-B. and Wang, Q.-H., *Fuel Process. Technol.*, 2001, vol. 72, p. 63.
4. Marquez-Montesinos, F., Cordero, T., Rodriguez-Mirasol, J., and Rodriguez, J.J., *Fuel*, 2002, vol. 81, p. 423.
5. Scott, S.A., Davidson, J.F., Dennis, J.S., and Hayhurst, A.N., *Proc. Combust. Inst.*, 2005, vol. 30, p. 2151.
6. Sinag, A., Sinek, K., Tekes, A.T., Misirlioglu, Z., Canel, M., and Wang, L., *Chem. Eng. Process.*, 2003, vol. 42, p. 1027.
7. Liu, H., Luo, Ch., Toyota, M., Kato, Sh., Uemiya, Sh., Kojima, T., and Tominaga, H., *Fuel*, 2003, vol. 82, p. 523.
8. DeGroot, W.F. and Shafizadeh, F., *Fuel*, 1984, vol. 63, p. 210.
9. RF Patent 2324647, 2008.
10. Bódi, T., Riba, D., Selmeci, J., and Török, I., *Energiagazdálkodás*, 1999, vol. 40, no. 3, p. 6.

11. Yoshida, S., Matsumami, J., Hosokawa, Y., Yokota, O., and Tamaura, Y., *Energy Fuels*, 1999, vol. 13, p. 961.
12. Kodama, T., Funatoh, A., Shimizu, K., and Kitayama, Y., *Energy Fuels*, 2001, vol. 15, p. 1200.
13. Kodama, T., Aoki, A., Shimizu, T., and Kitayama, Y., *Energy Fuels,* 1998, vol. 12, p. 775.
14. Kodama, T., *Prog. Energy Combust. Sci.*, 2003, vol. 29, p. 567.
15. Burroughs, C., Sandia News Releases. http://www.sandia.gov/news/resources/releases/2007/sunshine.html. Cited December 5, 2007.
16. Saber, J.M., Kester, K.B., Falconer, J.L., and Brown, L.F., *J. Catal.*, 1988, vol. 109, p. 329.
17. Iwaki, H., Ye, S., Katagiri, H., and Kitagawa, K., *Appl. Catal., A*, 2004, vol. 270, p. 237.
18. Ido, T., Mori, M., Jin, G., and Goto, S., *Kagaku Kogaku Ronbunshu*, 2001, vol. 27, no. 1, p. 121.
19. Gokon, N., Hasegawa, N., Kaneko, H., Aoki, H., Tamaura, Y., and Kitamaura, M., *Sol. Energy Mater. Sol. Cells*, 2003, vol. 80, p. 335.
20. Yamada, T., Tomita, T., Tamai, Y., and Homma, T., *Fuel*, 1983, vol. 62, p. 246.
21. Figueiredo, J.L., Rivera-Utrilla, J., and Ferro-Garcia, M.A., *Carbon*, 1987, vol. 25, p. 703.
22. Holstein, W.L. and Boudart, M., *Fuel*, 1983, vol. 62, p. 162.
23. Sugiura, K., Minami, K., Yamauchi, M., Morimitsu, S., and Tanimoto, K., *J. Power Sources*, 2007, vol. 171, p. 228.
24. Bulgarian Patent 51785, 1993.
25. Figueiredo, J.L., Orfao, J.J.M., and Ferraz, M.C.A., *Fuel*, 1984, vol. 63, p. 1059.
26. Skodras, G. and Sakellaropoulos, G.P., *Fuel Process. Technol.*, 2002, vol. 77, p. 151.
27. Fedoseev, S.D., *Kinetika i diffuziya v porakh uglerodnogo materiala* (Kinetics and Diffusion in Pores of a Carbon Material), Moscow: Mosk. Khim.–Tekhnol. Inst., 1988.
28. Shelekhov, E.V. and Sviridova, T.A., *Metalloved. Term. Obrab. Met.*, 2000, no. 8, p. 16.
29. *Kratkii spravochnik fiziko-khimicheskikh velichin* (Concise Handbook of Physical and Chemical Quantities), Mishchenko, K.P. and Ravdel', A.A., Eds., Leningrad: Khimiya, 1974.
30. US Patent 0095693, 2008.
31. RF Patent 2319664, 2008.
32. Bychkov, V.Yu., Krylov, O.V., and Korchak, V.N., *Kinet. Catal.*, 2002, vol. 43, p. 86.
33. Reznik, D., Olk, C.H., Neumann, D.A., and Copley, J.R.D., *Phys. Rev. B: Condens. Matter,* 1995, vol. 52, p. 116.
34. Kuijpers, E.G.M. and Geus, J.W., *Fuel,* 1983, vol. 62, p. 158.
35. Krivoruchko, O.P. and Zaikovskii, V.I., *Kinet. Catal.*, 1998, vol. 39, p. 561.
36. Harris, P.J.F., *Carbon Nanotubes and Related Structures*, Cambridge: Cambridge Univ. Press, 1999.
37. Karaeva, A.R., Dolgova, E.A., Kharitonov, D.N., Maslov, I.A., Kamenev, A.A., Tret'yakov, V.F., and Mordkovich, V.Z., *Ros. Khim. Zh.*, 2006, vol. 1, no. 1, p. 64.
38. Figueiredo, J.L., Bernardo, C.A., Chludzinski, J.J.., and Baker, R.T.K., *J. Catal.*, 1988, vol. 110, p. 127.
39. Tavares, M.T., Astrup, I., Bernardo, C.A., and Rostrup-Nielsen, J.R., *J. Catal.*, 1994, vol. 147, p. 525.
40. Bukharkina, T.V., Verzhichinskaya, S.V., Digurov, N.G., and Tumanyan, B.P., *Khimiya prirodnykh energonositelei i uglerodnykh materialov* (Chemistry of Natural Energy Carriers and Carbon Materials), Moscow: Tekhnika, 2009.
41. Chesnokov, V.V. and Buyanov, R.A., *Usp. Khim.*, 2000, vol. 69, p. 675.
42. Baker, R.T.K., Chludzinski, J.J., and Sherwood, R.D., *Carbon*, 1985, vol. 23, p. 245.
43. Bychkov, V.Yu., Tyulenin, Yu.P., Krylov, O.V., and Korchak, V.N., *Kinet. Catal.*, 2002, vol. 43, p. 724.
44. Silva, L.M.S., Orfao, J.J.M., and Figueiredo, J.L., *Appl. Catal.*, 2001, vol. 209, p. 145.
45. Emmanuel, N.M. and Knorre, D.G., *Kurs khimicheskoi kinetiki* (Chemical Kinetics), Moscow: Vysshaya Shkola, 1984.
46. Hansen, M. and Anderko, K., *Constitution of Binary Alloys,* New York: McGraw-Hill, 1957.
47. Bychkov, V.Yu., Tyulenin, Yu.P., and Korchak, V.N., *Kinet. Catal.*, 2003, vol. 44, p. 353.
48. Tyulenin, Yu.P., Savkin, V.V., Sinev, M.Yu, and Korchak, V.N., *Kinet. Catal.*, 2002, vol. 43, p. 847.
49. Colle, K.S., Kim, K., and Wold, A., *Fuel*, 1983, vol. 62, p. 155.